The solar coronal magnetic field

Thomas Wiegelmann

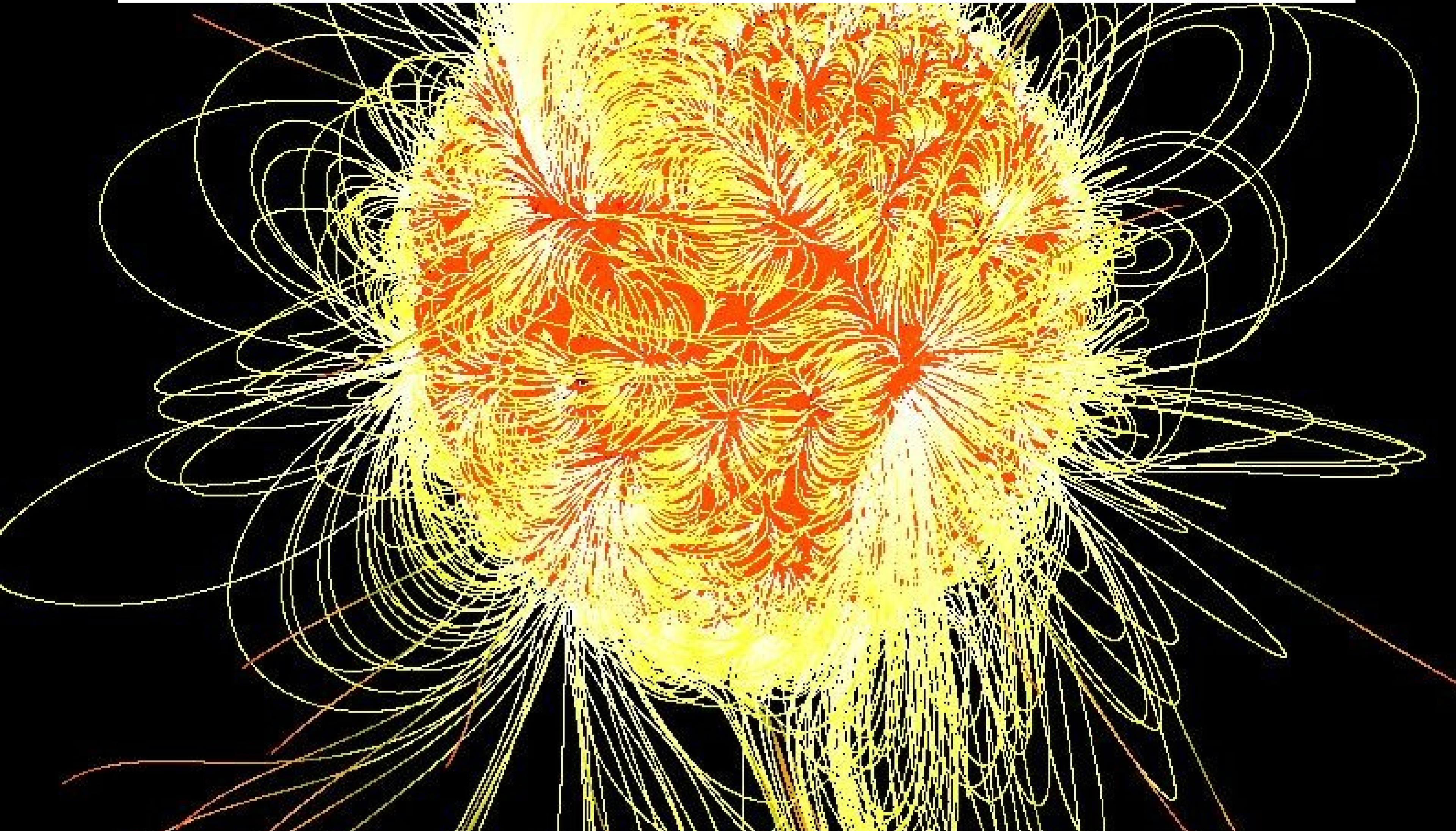

Solar Corona is very dynamic

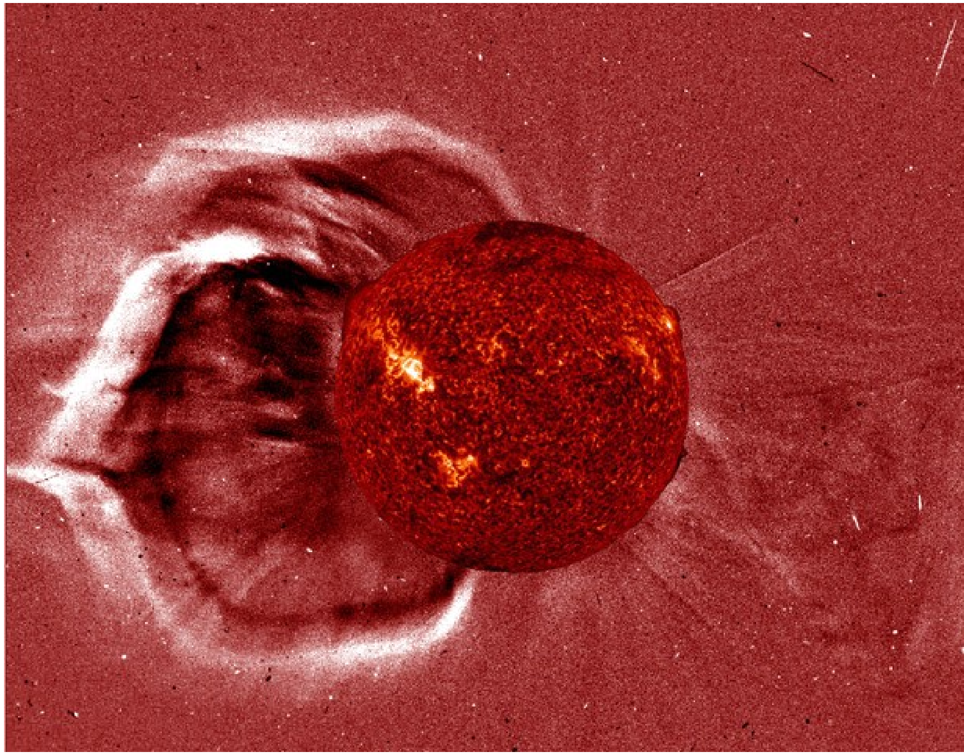

Coronal mass ejection on August, 10 2010. Composite image from SDO

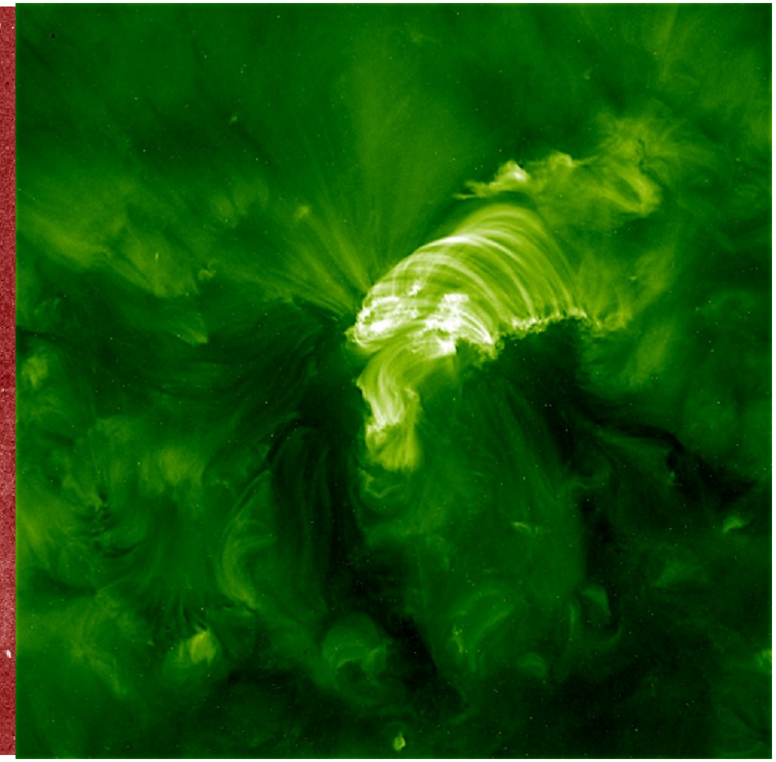

An AIA image in 193 Å after a solar eruption and a flare.

Source: http://sdo.gsfc.nasa.gov/gallery

Eruption have impact on Earth

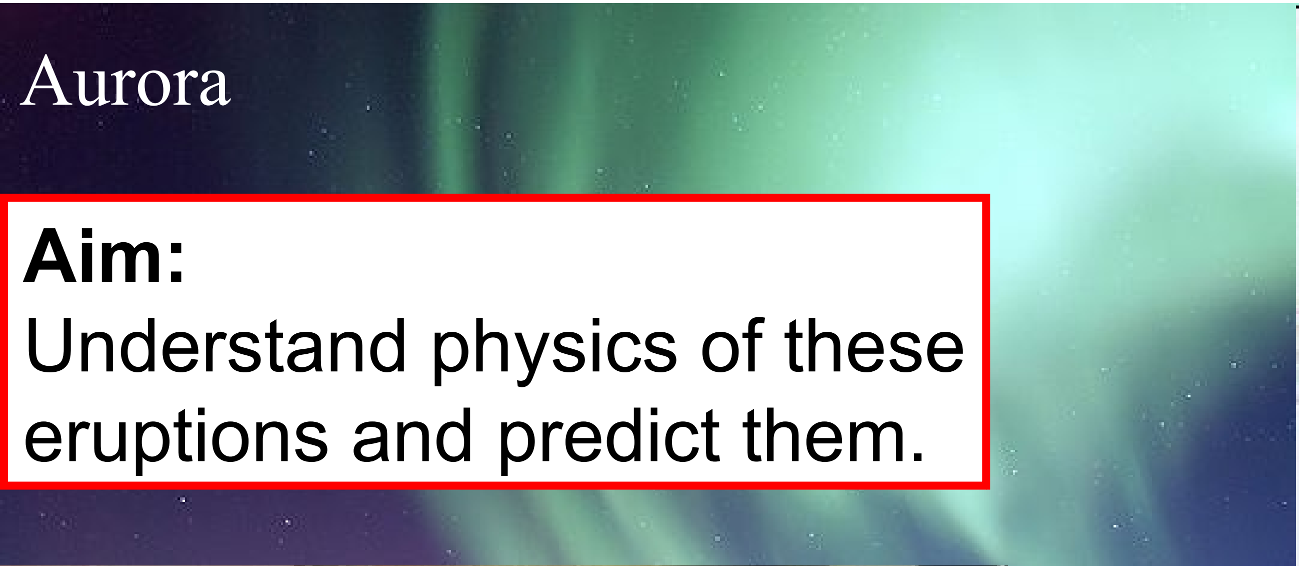

Aim:
Understand physics of these eruptions and predict them.

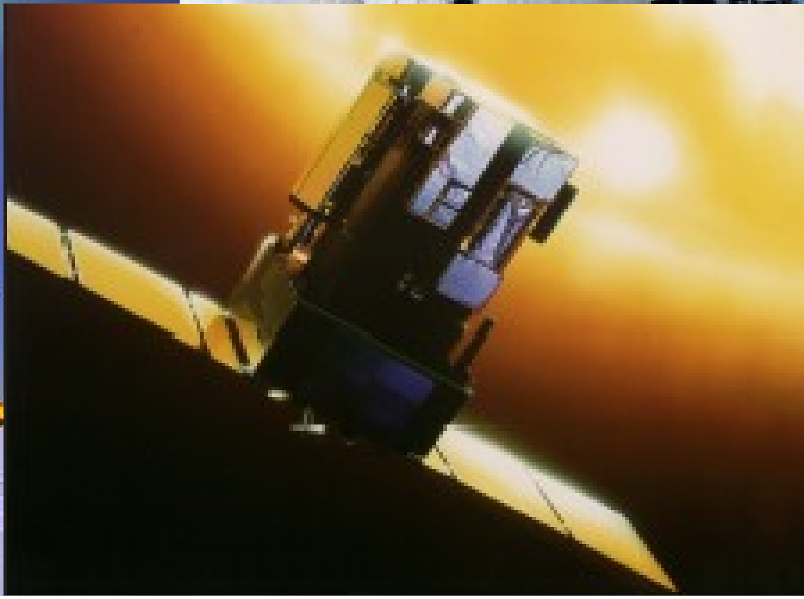

Solar magnetic fields: Measurements and Impact

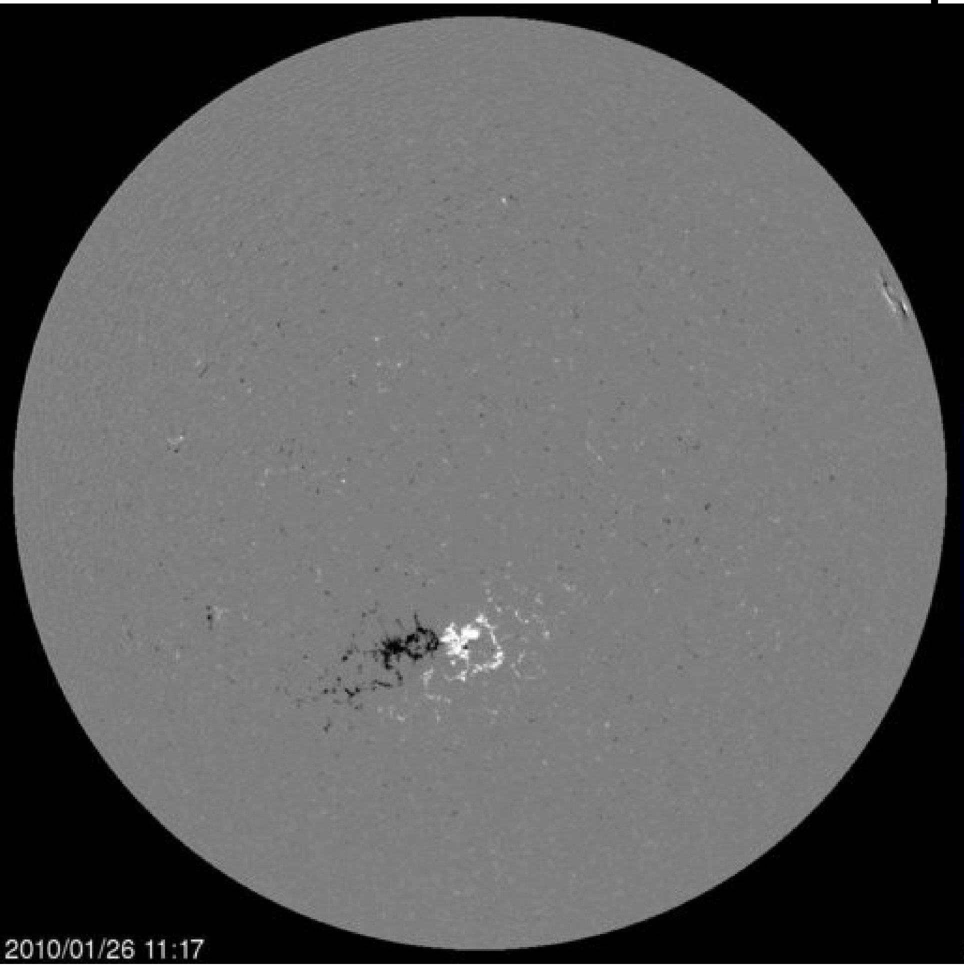

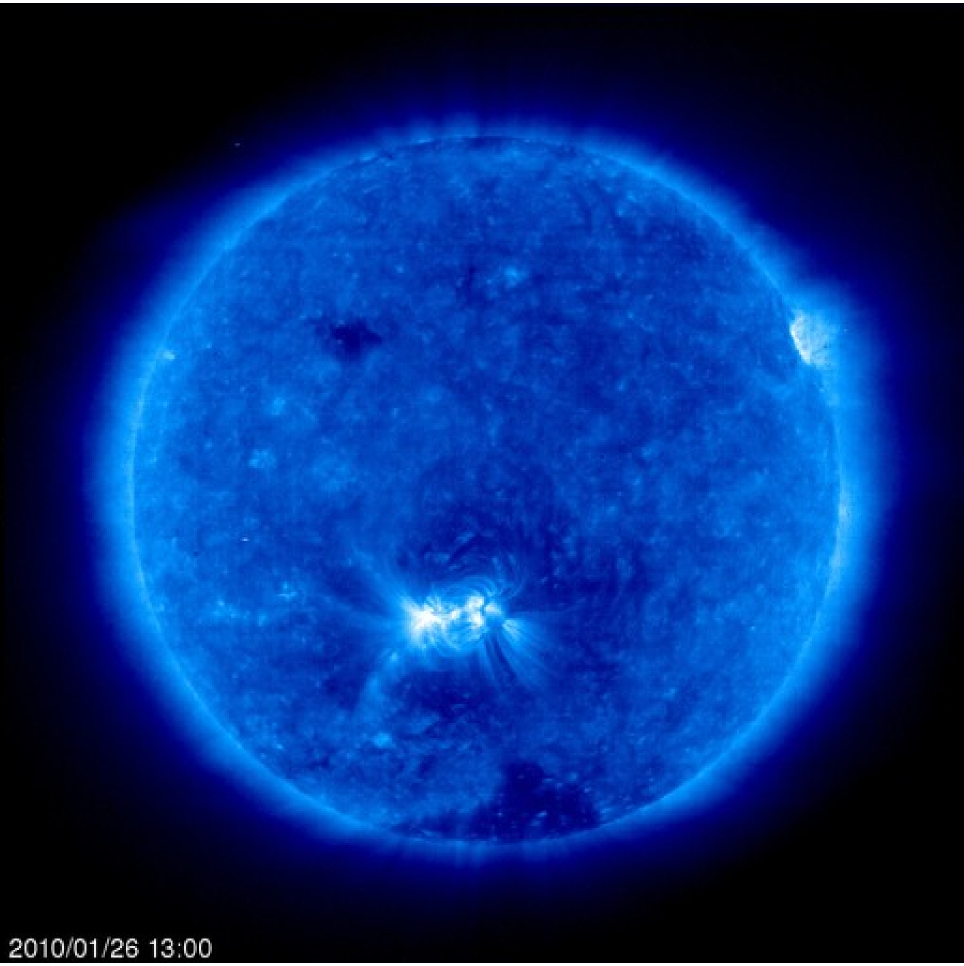

Magnetic fields are measured routinely in the Solar photosphere **(SOHO/MDI).**

Magnetic fields structure the coronal plasma (SOHO/EIT).

We „see“ field lines in
coronal EUV-images

We measure the magnetic field in photosphere

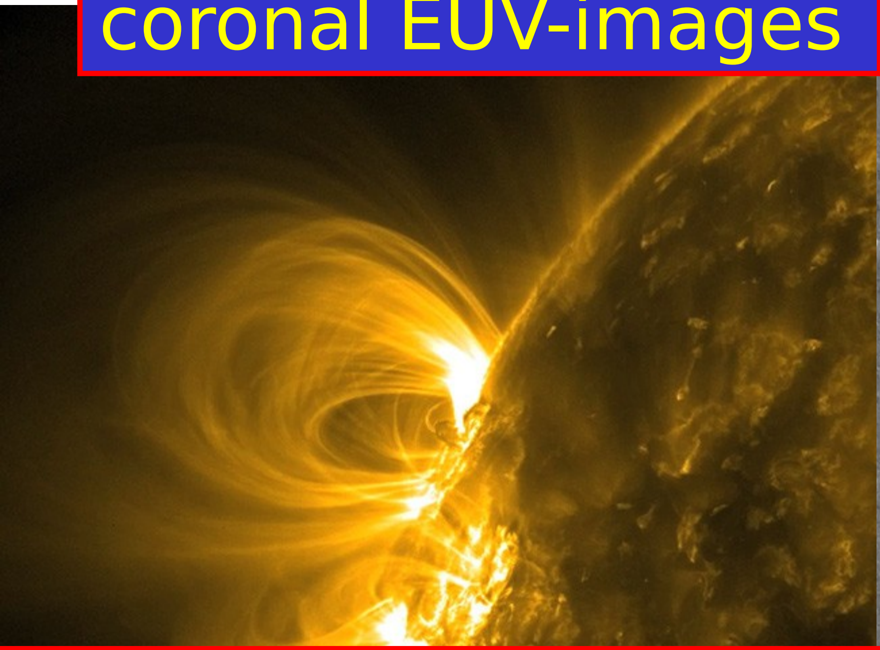

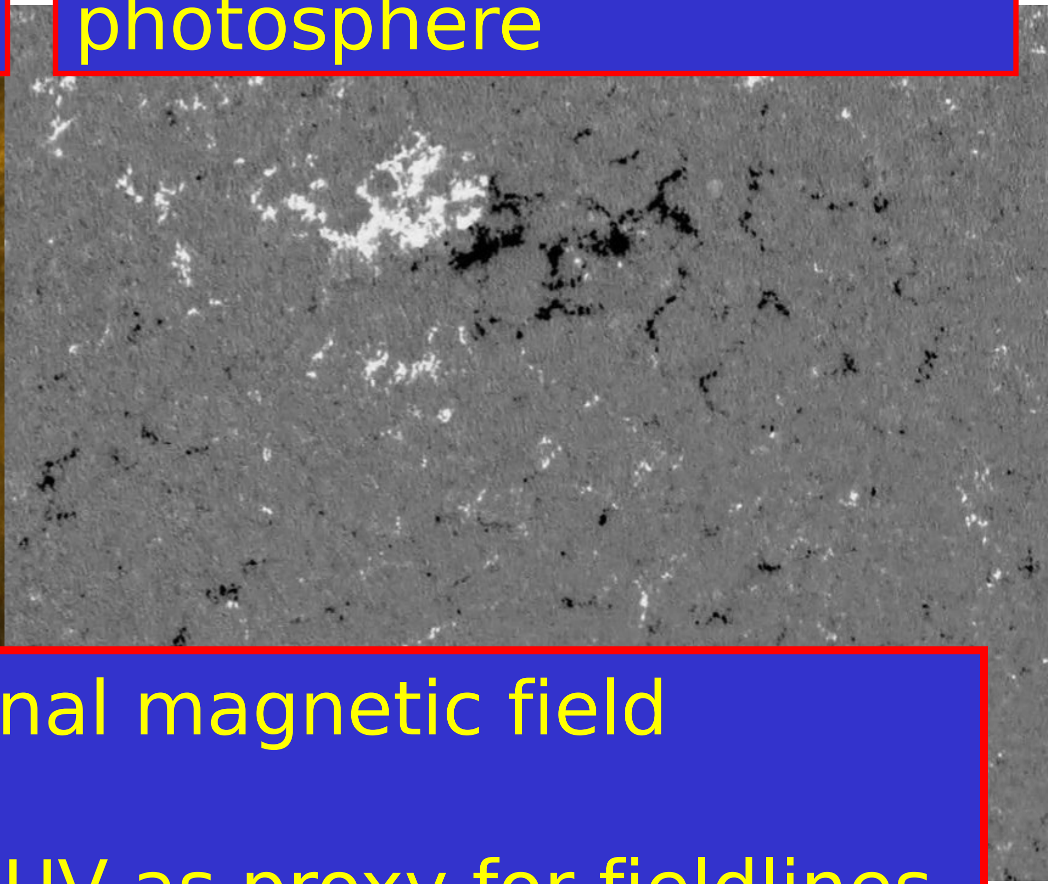

How to derive the coronal magnetic field structure?

1. Use loops visible in EUV as proxy for fieldlines
=> Stereoscopy to derive 3D structure
2. Extrapolate photospheric field vector in the corona

1.) Stereoscopy, Stereo mission

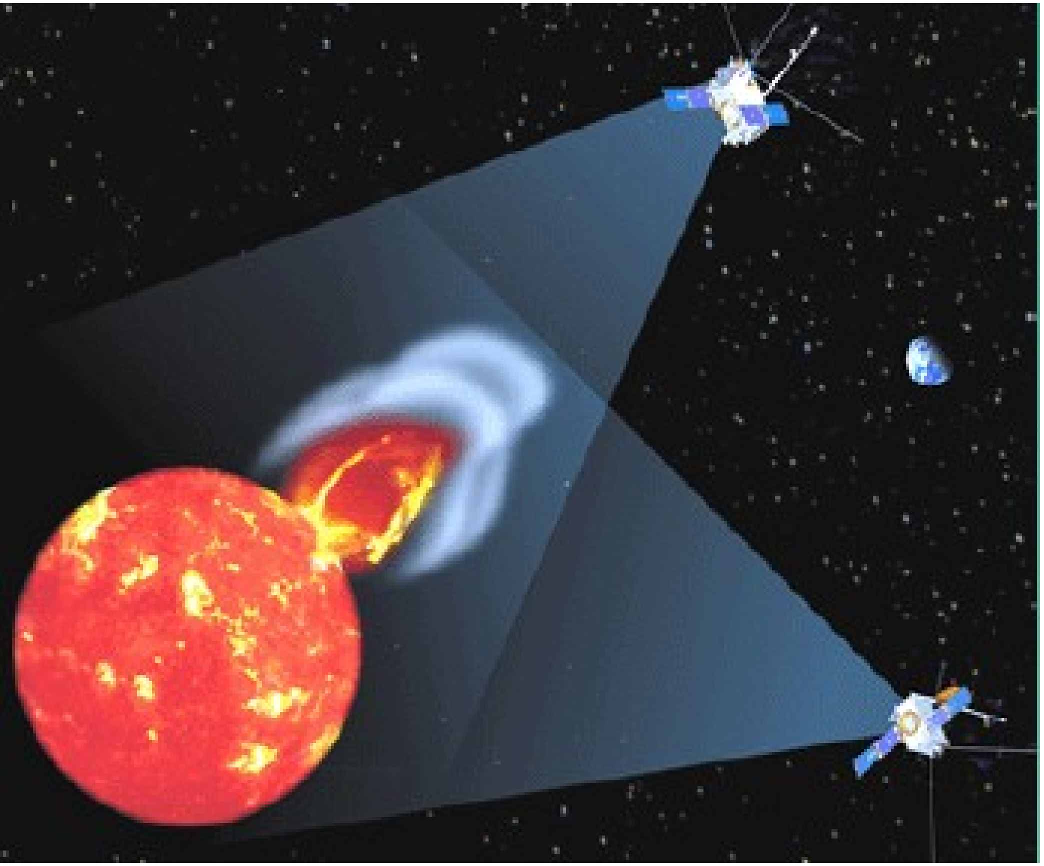

The 2 STEREO-
spacecraft
observe the Sun
simulta-
neously. For oberserving
(plama on) magnetic
field lines, we use
mainly
EUV-images from
STEREO/SECCHI.

SOHO/EIT and SDO/AIA
can be used as third
eye.

Associate objects in both images: The correspondence problem

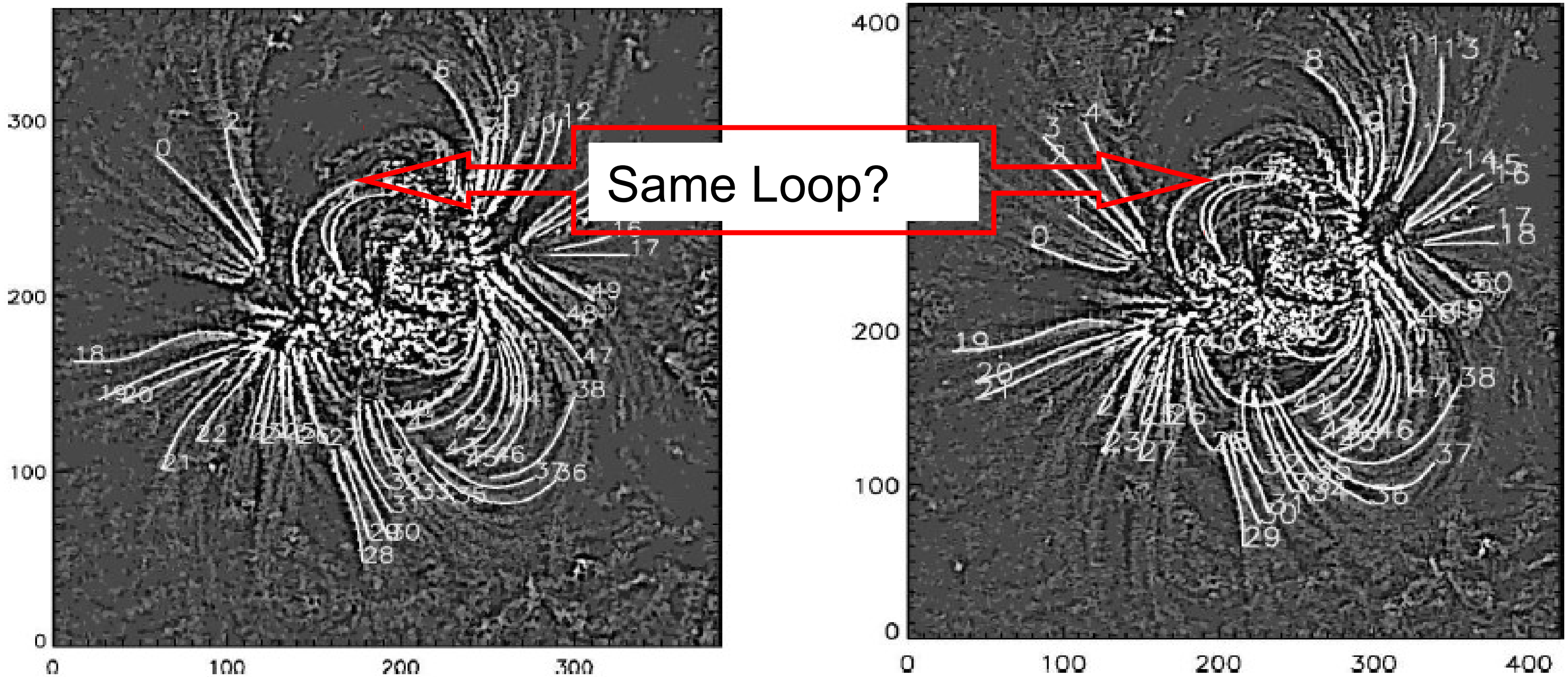

Contrast enhanced EUVI-images from STEREO-A (right) and B. Overplotted are automatic extracted loops. Same number in both images do not neccessarily correspond t the same loop. (From Feng et al., ApJL 2007)

Geometric stereoscopy

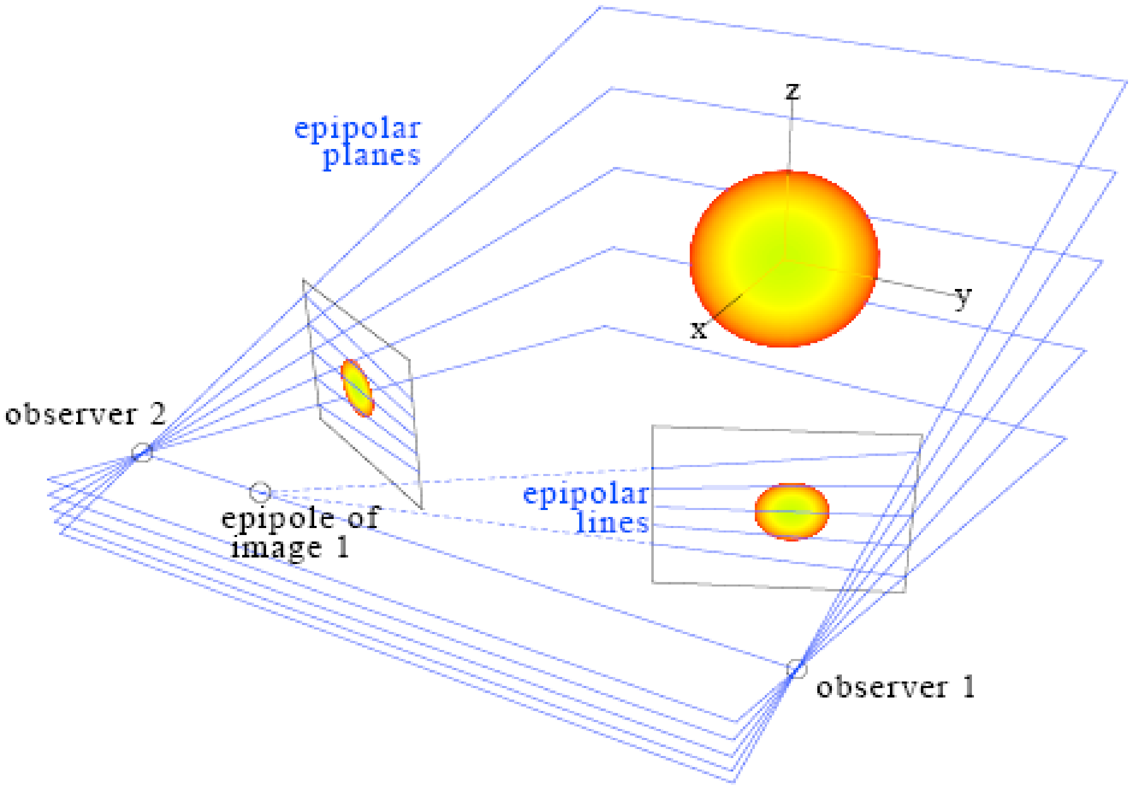

From Inhester,
ISSI 2006

Reconstruction error

Stereo-angle 3.4 degree
red: direct stereoscopy
black: spline fit

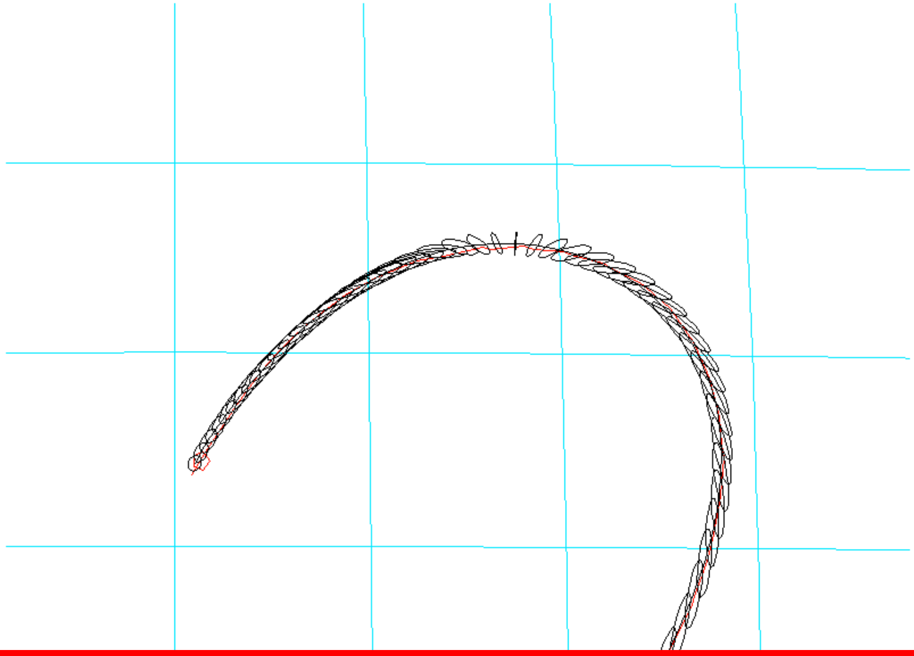

- Features tangential to epipolar lines have highest reconstruction error.
- For east-west coronal loops this means that largest reconstruction errors occur at the loop top.

2. Extrapolate photospheric fields: Force-free coronal magnetic fields

In the coronal low beta plasma we can neglect in lowest order non-magnetic forces like pressure gradients and gravity and derive the (usually nonlinear) **force-free field equations**:

$$
\begin{aligned}
(\nabla \times \mathbf{B}) \times \mathbf{B} &= \mathbf{0}, \\
\nabla \cdot \mathbf{B} &= 0.
\end{aligned}
$$

A subclass of force-free fields are current free potential fields

$$\nabla \times \mathbf{B} = 0 \qquad \nabla \cdot \mathbf{B} = 0 \quad \Rightarrow \quad \mathbf{B} = \nabla \Phi \qquad \Delta \Phi = 0$$

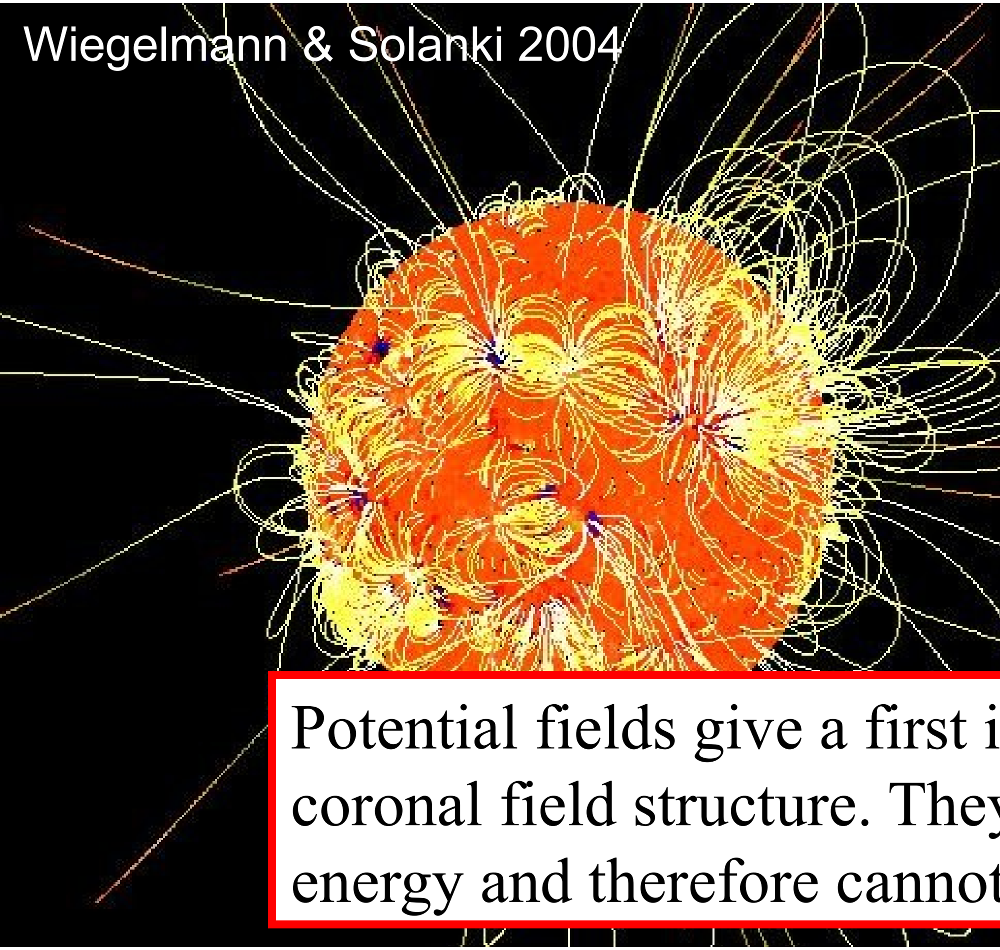

Potential fields give a first impression on the global coronal field structure. They do not contain free energy and therefore cannot erupt.

Global Potential fields (SOHO/MDI) Plasma in (SOHO/ EIT)

NonLinear Force-Free Fields

$$(\nabla \times \mathbf{B}) \times \mathbf{B} = \mathbf{0}$$
$$\nabla \cdot \mathbf{B} = 0$$

Equivalent

$$\nabla \times \mathbf{B} = \alpha \mathbf{B}$$
$$\mathbf{B} \cdot \nabla \alpha = 0$$

- Compute initial a potential field
  (Requires only Bn on bottom boundary)
- Iterate for NLFFF-field, Boundary conditions:
  - Bn and Jn for positive or negative polarity on boundary (**Grad-Rubin method**)
  - Magnetic field vector Bx By Bz on boundary (**MHD-relaxation**, **Optimization method**)

Consistent boundary conditions for force-free fields

(Molodensky 1969, Aly 1989)

$$\int_V \nabla \cdot \mathbf{B} \, d^3x = 0 \Rightarrow \oint_S \mathbf{B} \, d\mathbf{S} = 0$$

Flux-balance

$$\int_V (\nabla \times \mathbf{B}) \times \mathbf{B} \, d^3x = 0$$

$$\int_V \nabla \cdot T \, d^3x = 0 \Rightarrow \oint_S T d\mathbf{S} = 0$$

$$T_{ij} = B_i B_j - \frac{1}{2}\mathbf{B}^2 \delta_{ij}$$

Maxwell Stress Tensor

No net force on boundary

$$\int_V \mathrm{r} \times [(\nabla \times \mathbf{B}) \times \mathbf{B}] \, d^3x = 0$$

$$\int_V \nabla \cdot \tilde{T} \, d^3x = 0 \Rightarrow \oint_S \tilde{T} d\mathbf{S} = 0$$

$$\tilde{T}_{ij} = \epsilon_{jkl} \, r_k \, T_{ij}$$

No net torque on boundary

Magnetic field is measured routinely in the photosphere. Other boundaries are a priori unknown.

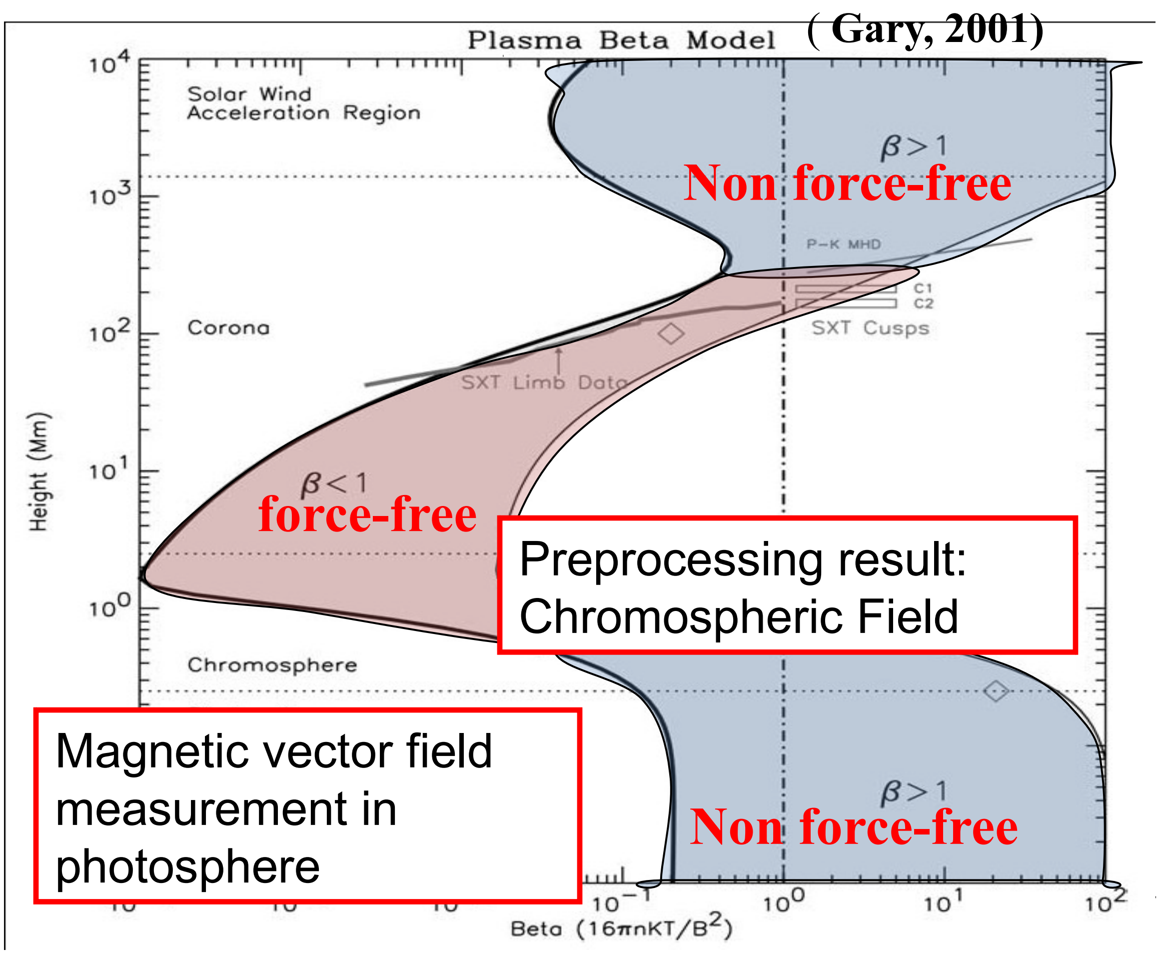

Preprocessing result:
Chromospheric Field

Magnetic vector field measurement in photosphere

If these relations are not fulfilled in the bottom boundary, force-free fields do not exist for these boundary conditions.

Possible Solution:
Use these relations to derive consistent boundary conditions for force-free coronal magnetic field models.

⇨ **Preprocessing**

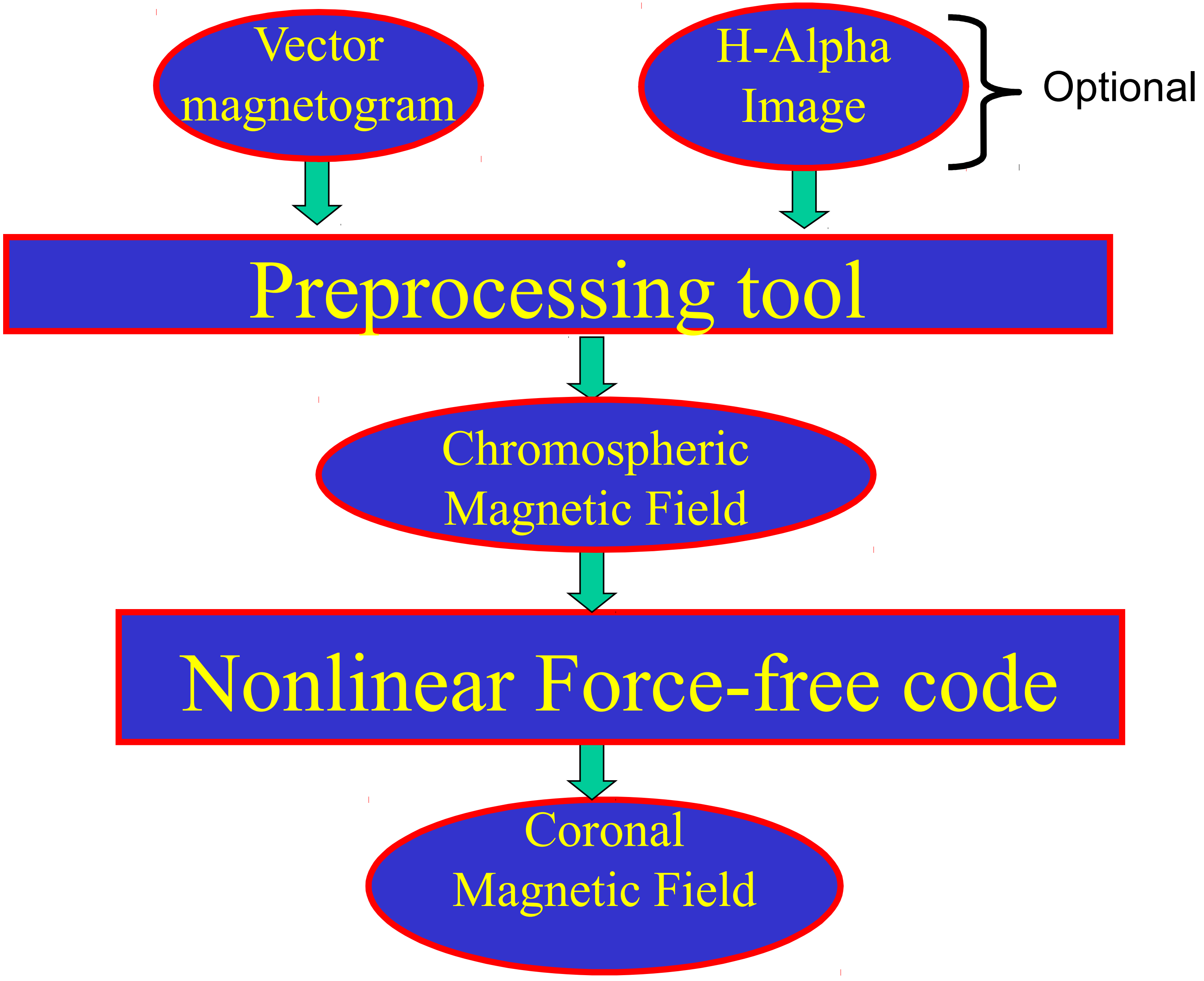
Vector magnetogram
H-Alpha Image
Optional
Preprocessing tool
Chromospheric Magnetic Field
Nonlinear Force-free code
Coronal Magnetic Field

Solar Flare Telescope, Tokyo

- Click to edit Master text styles
  - Second level
    - Third level
      - Fourth level
        - Fifth level

Application to 2 Active Regions
(Thalmann et al. 2008)

vector magnetograph data : field of view

January 2004 : AR 10540 – SFT/VM

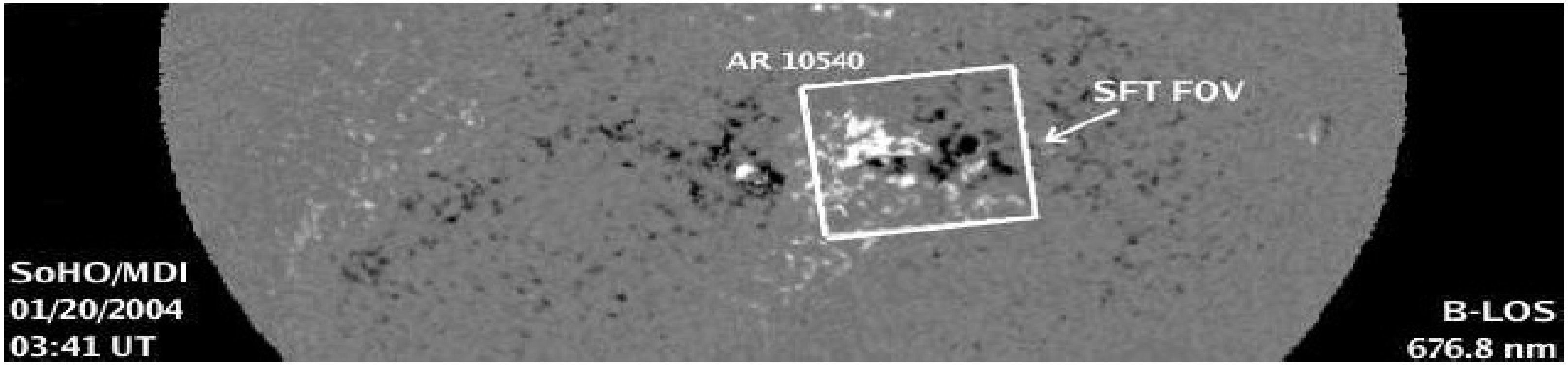

June 2007 : AR 10960 – SOLIS/VSM

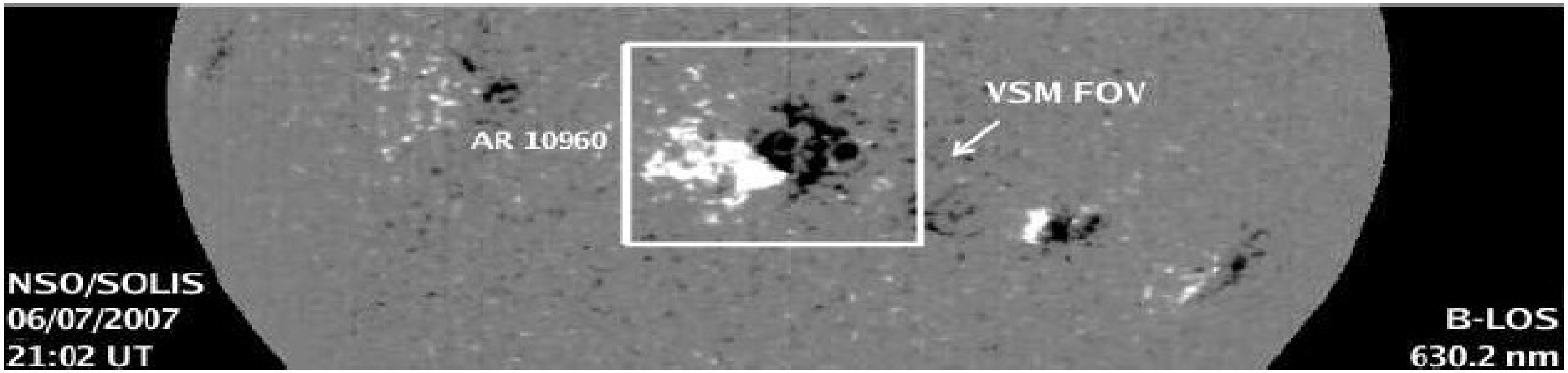

Flaring Active Region

Quiet Active Region

Magnetic energy builds up and is releases during flare

M Flare

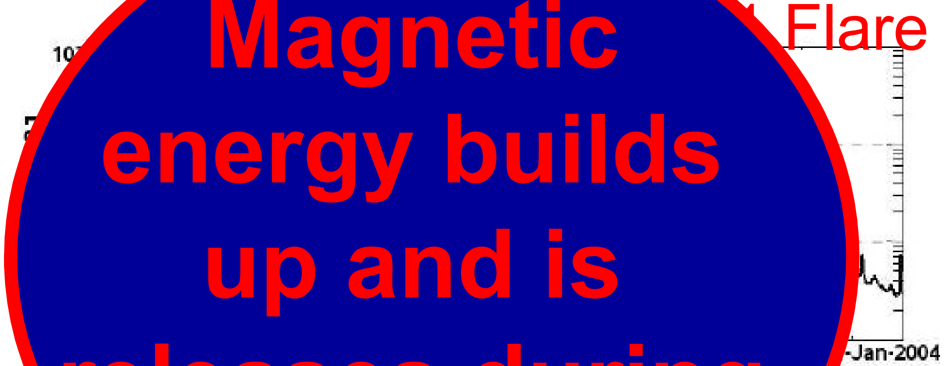

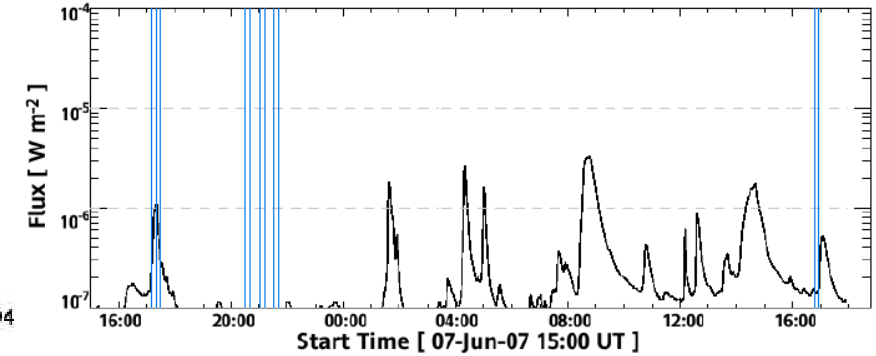

ue lines: vector magnetograms available

M6.1 Flare

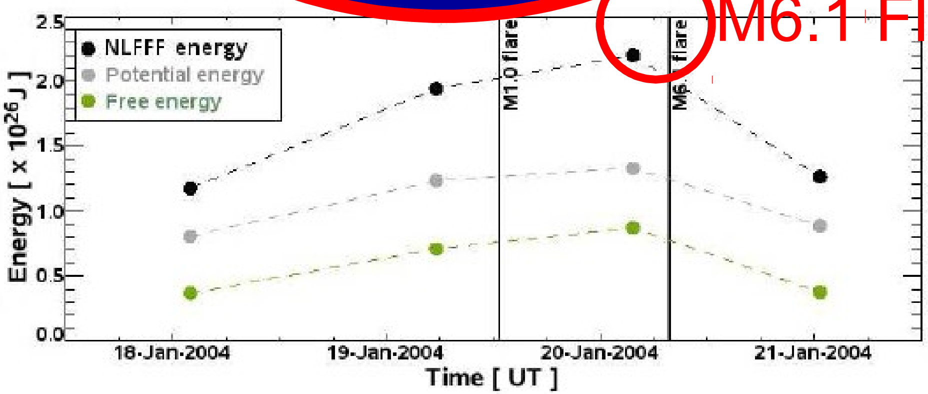

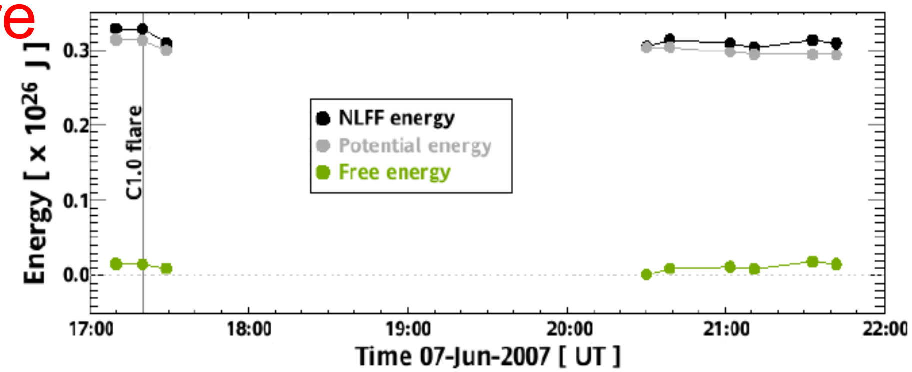

Magnetic field extrapolations
from Solar Flare telescope

Extrapolated from SOLIS
vector magnetograph

Stereoscopy vs. force-free field extrapolation

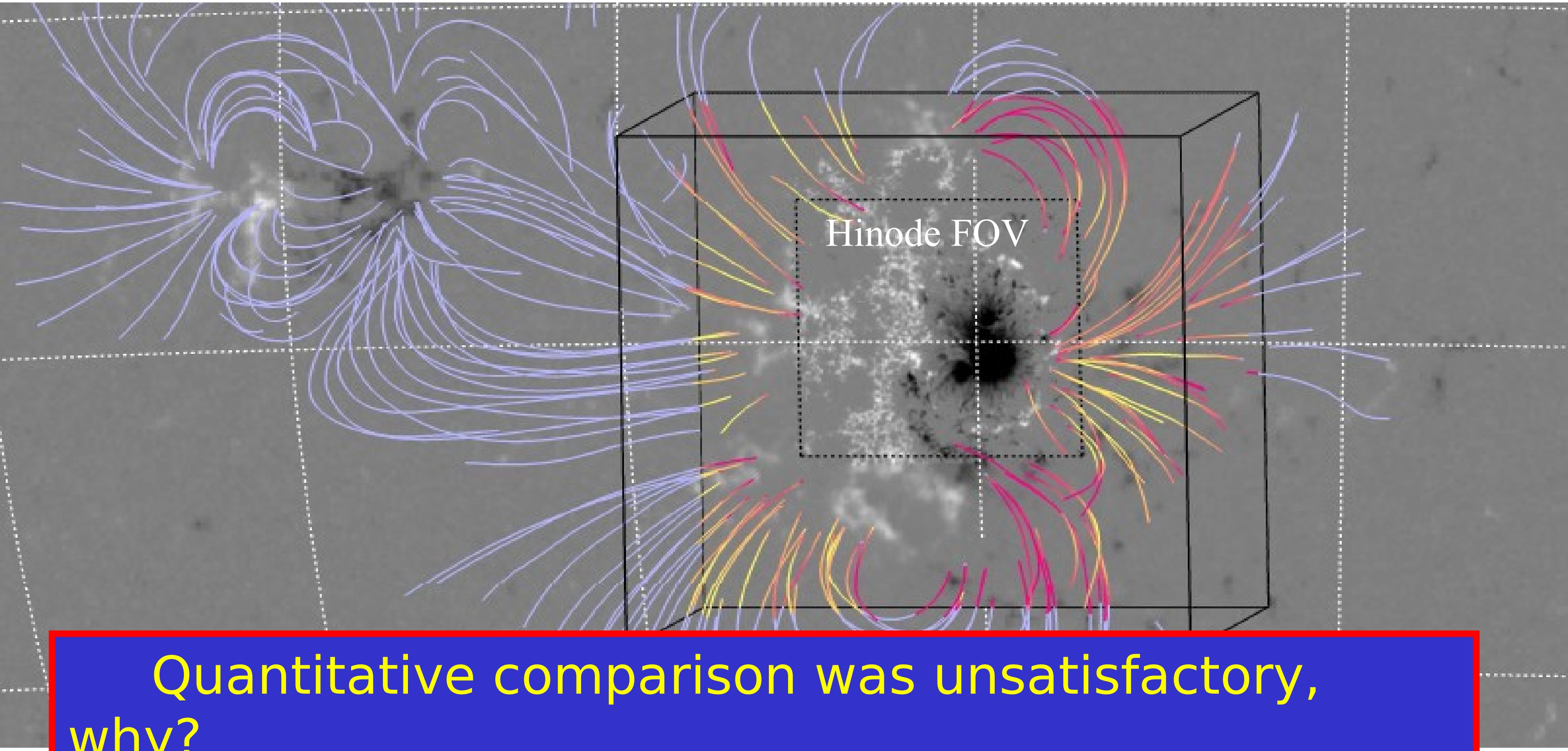

Quantitative comparison was unsatisfactory, why?

- Limited FOV of Hinode-vector magnetograms
- Error in stereoscopy-loops due to small separation angle between STEREO-spacecraft.

What to do? Joint suggestions from NLFFF-workshops, DeRosa et al. ApJ, 2009

Successful use of nonlinear force-free models require:

1. large model volumes at high resolution that accommodate most of the connectivity within a region and to its surroundings;
2. accommodation of measurement uncertainties (in particular in the transverse field component) in boundary condition;
3. 'preprocessing' of the lower-boundary vector field for a realistic approximation of the high-chromospheric, near force-free field;
4. Force-free models should be compared (or even improved) with coronal observations.

SDO/HMI

Done, next slide

Routinely done with SDO/AIA

NLFFF optimization code

$$(\nabla \times \mathbf{B}) \times \mathbf{B} = \mathbf{0}$$

$$\nabla \cdot \mathbf{B} = 0$$

$$\mathbf{B} = \mathbf{B}_{\mathrm{obs}} \text{ on bottom boundary}$$

$$L = \int_V w_f \frac{|(\nabla \times \mathbf{B}) \times \mathbf{B}|^2}{B^2} + w_d \, |\nabla \cdot \mathbf{B}|^2 \, d^3V$$

$$+\nu \int_S (\mathbf{B} - \mathbf{B}_{obs}) \cdot \mathbf{W} \cdot (\mathbf{B} - \mathbf{B}_{obs}) d^2S$$

grangian multiplier and mask have to be optimized

The SDO-era (since 2010)

How to optimize an NLFFF-code for active regions observed with HMI?

R 11158, observed 14. Feb. 2011
MI-vector data for testing

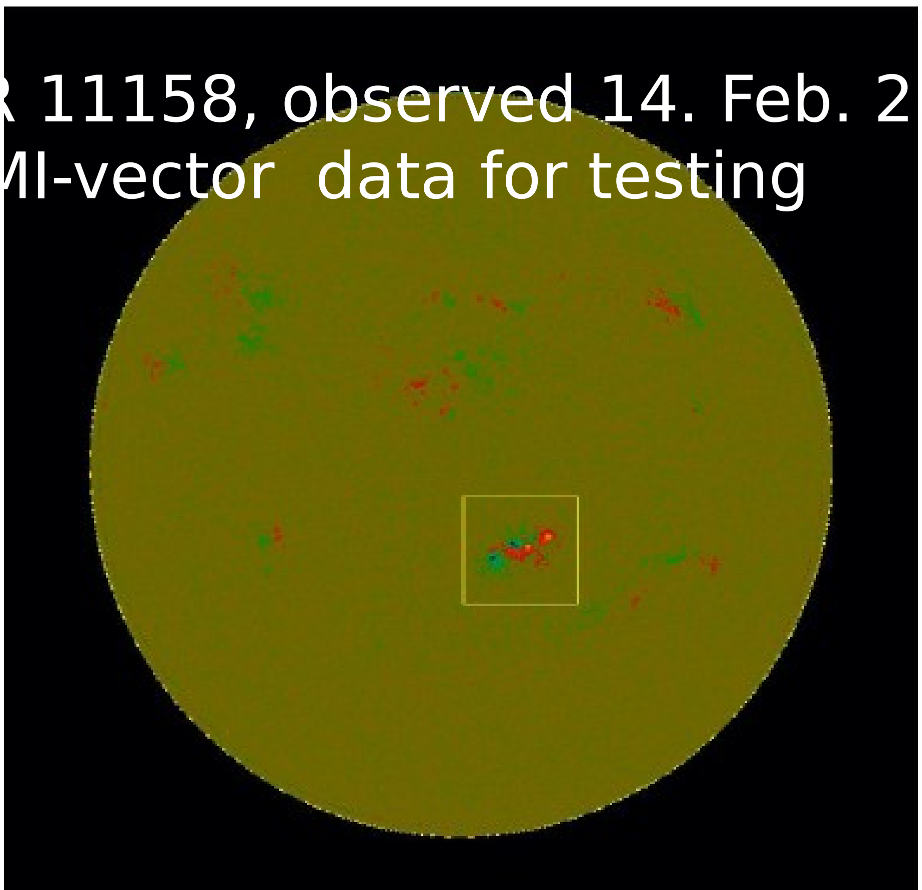

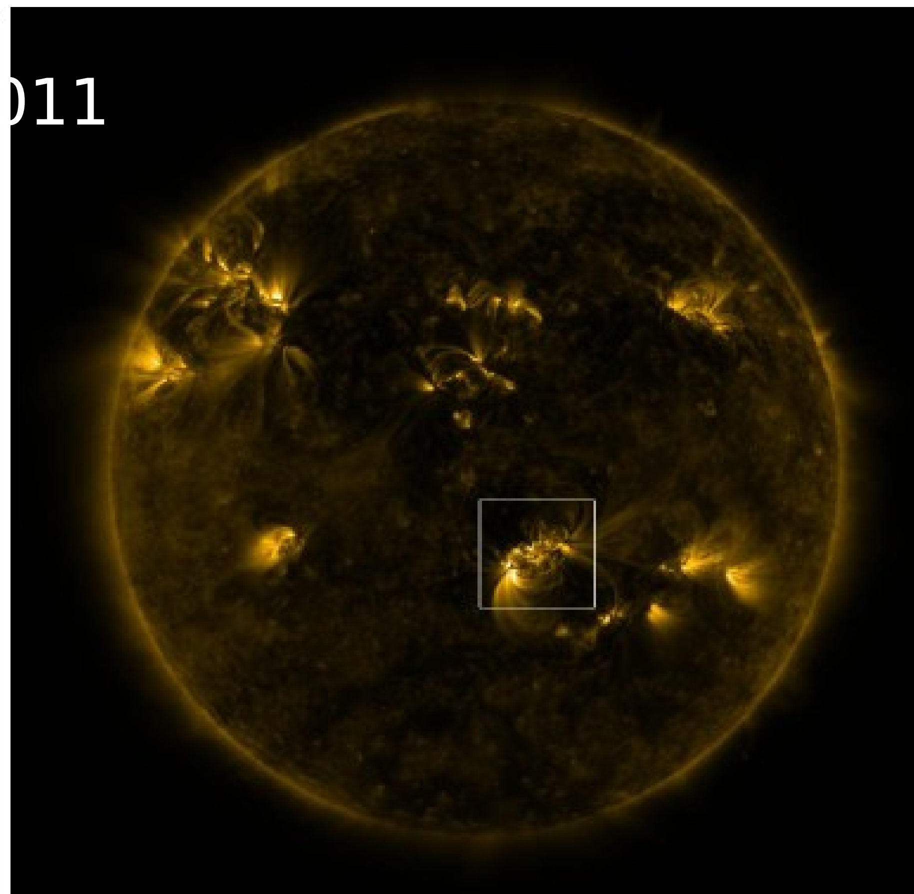

Quality of the vector magnetogram (consistency with force-free model)

$$\epsilon_{\text{flux}} = \frac{\int_S B_z}{\int_S |B_z|}$$

$$\epsilon_{\text{force}} = \frac{|\int_S B_x B_z| + |\int_S B_y B_z| + |\int_S (B_x^2 + B_y^2) - B_z^2|}{\int_S (B_x^2 + B_y^2 + B_z^2)}$$

$$\epsilon_{\text{torque}} = \frac{|\int_S x((B_x^2 + B_y^2) - B_z^2)| + |\int_S y((B_x^2 + B_y^2) - B_z^2)| + |\int_S yB_xB_z - xB_yB_z|}{\int_S \sqrt{x^2 + y^2}\ (B_x^2 + B_y^2 + B_z^2)}$$

These quantities should be small on the bottom boundary of a NLFFF-simulation Box.
If this is not the case
=>Preprocessing (Wiegelmann et al. 2006)

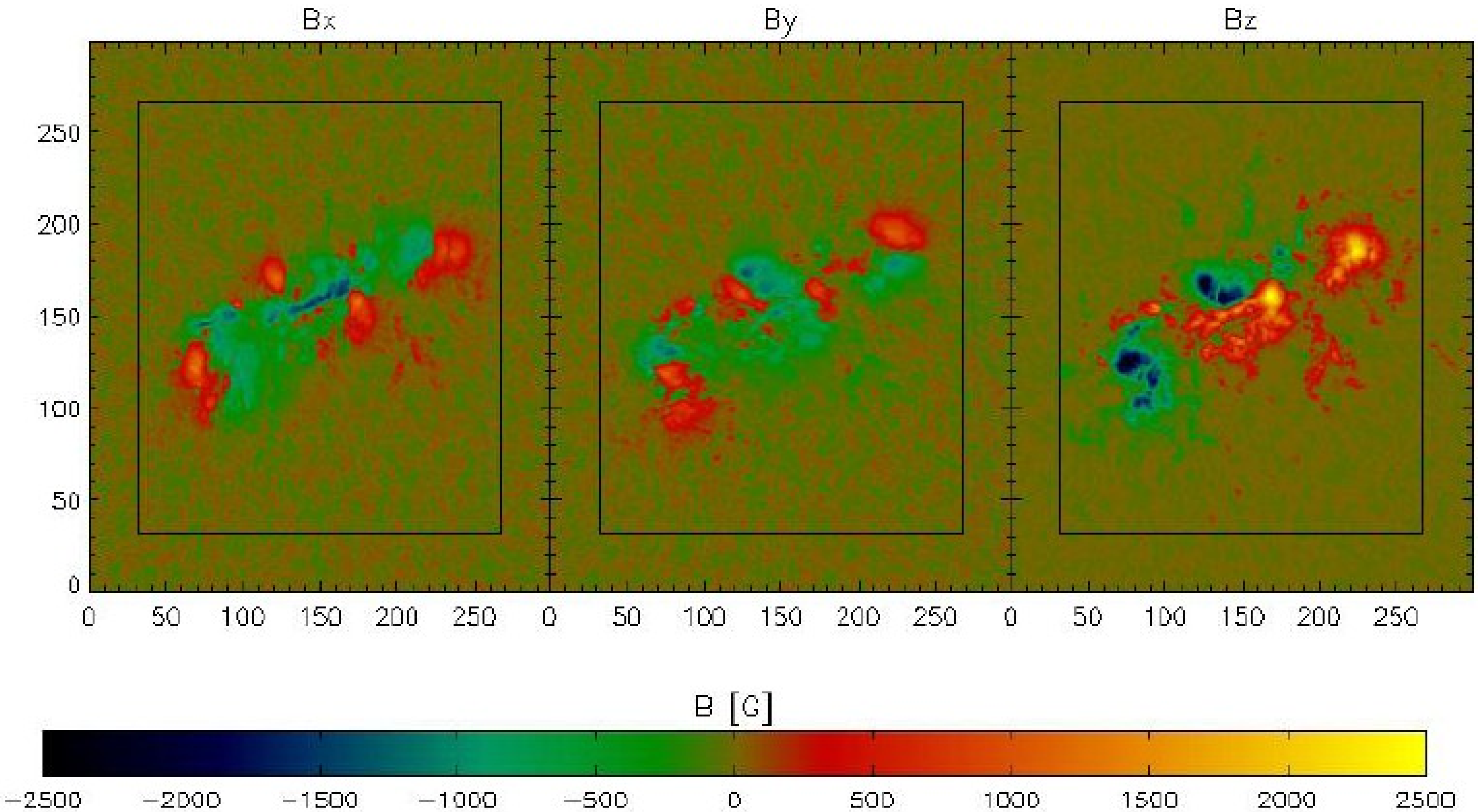

Data set	ϵ_{flux}	ϵ_{force}	ϵ_{torque}
HMI, Feb.14 2011	0.0034	0.0564	0.0535
preprocessed HMI	0.0037	0.0002	0.0009
SFT Oct.26 1992	0.0854	0.6842	0.8837
Hinode Dec.12 2006	0.0167	0.2727	0.3387
SOLIS Jun.07 2007	0.0124	0.6400	0.6691

HMI-Vecmag is almost force-free. For this AR or in general? We do not know.

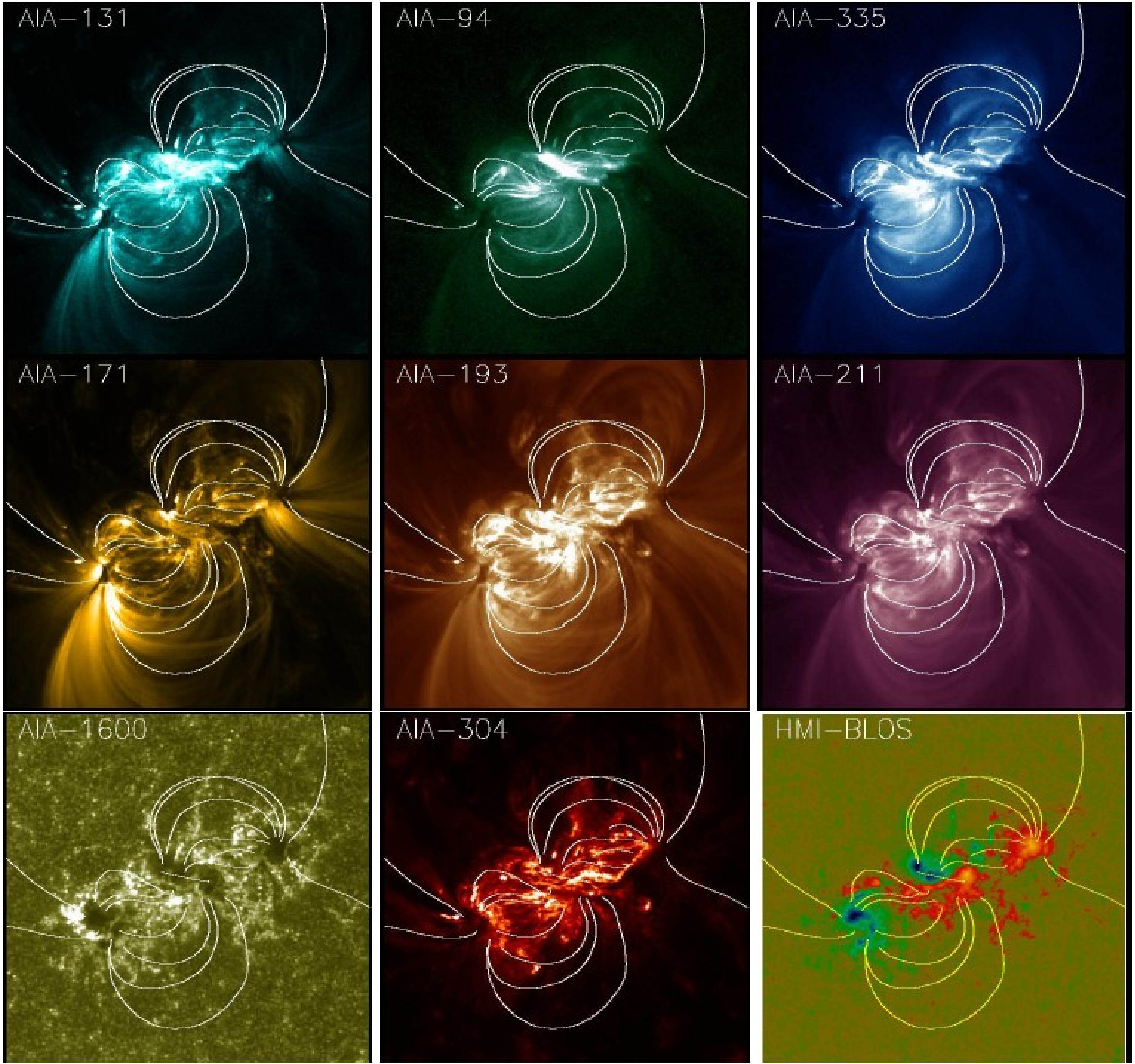

AIA−131
AIA−94
AIA−335
AIA−171
AIA−193
AIA−211
AIA−1600
AIA−304
HMI−BLOS

Conclusions

- With EUV-images from several viewpoints we get 3D topology of loops and plasma parameters.
- State of the art of magnetic field extrapolations are non-linear force-free models.
- Both methods have shortcomings/errors and we should continue to compare and combine
  them, e.g. with SDO/AIA and HMI.


THANK YOU